THE JOURNAL OF PHYSICAL CHEMISTRY B

Article

pubs.acs.org/JPCB

Water and Membrane Dynamics in Suspensions of Lipid Vesicles Functionalized with Poly(ethylene glycol)s

Eduardo M. Clop,[†] Ana K. Chattah,[‡] and María A. Perillo*,[†]

[†]IIByT (CONICET-UNC), Cátedra de Química Biológica, Facultad de Ciencias Exactas Físicas y Naturales, Universidad Nacional de Córdoba, Av. Vélez Sarsfield 1611, X5016GCA Córdoba, Argentina

[‡]Facultad de Matemática Astronomía y Física (FaMAF) and IFEG (CONICET-UNC), Universidad Nacional de Córdoba, Ciudad Universitaria, X5016LAE Córdoba, Argentina

ABSTRACT: The present work was aimed at studying the molecular dynamics at different levels of model membranes having a simulated glycoclix, with focus on the molecular crowding conditions at the lipid−water interfacial region. Thus, binary mixtures of dipalmitoylphosphatidylcholine (dpPC) and a poly(ethylene glycol) (PEG^n) derivative of dipalmitoylphosphatidylethanolamine (PE) (where n = 350, 1000, and 5000, respectively, refer to PEG molecular masses) were submitted to ^{1}H spin−lattice relaxation time (T_1) and ^{31}P NMR spectra analysis. ^{1}H NMR relaxation times revealed two contributing components in each proton system (PEG, phospholipids, and water), for all the mixtures studied, exhibiting values of T_1 with very different orders of magnitude. This allowed identifying confined and bulk water populations as well as PEG moieties becoming more disordered and independent from the phospholipid moiety as n increased. ^{31}P spectra showed a typical broad bilayer signal for n = 350 and 1000, and an isotropic signal characteristic of micelles for n = 5000. Surface pressure (π)−molecular area isotherms and compressional modulus measurements provided further structural information. Moreover, epifluorescence microscopy data from monolayers at $\pi \sim 30$ mN/m, the expected equilibrium π in lipid bilayers, allowed us to postulate that both ^{1}H populations resolved through NMR in phospholipids and lipopolymers corresponded to different phase domains.

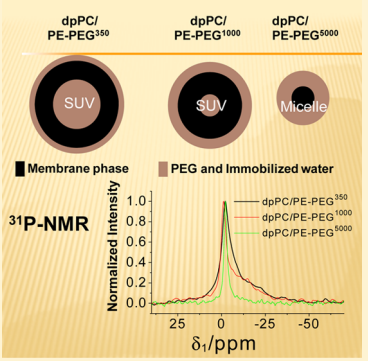

INTRODUCTION

Biochemical processes occur at a high global concentration of macromolecules, between 50 and 400 mg/mL (5−40% W/V).[1−3] This is a distinguishing feature of living systems usually described as molecular crowded (MC) environments. Within MC media, macromolecules occupy a large fraction of volume that cannot be occupied by other molecules.[4] Thus, large molecules are confined due to their big size compared with the pore size[5,6] and the volume accessible to small molecules is significantly lower than under conditions of dilute solutions, where most experiments are done. As a result, molecules are subjected to steric and diffusional restrictions affecting their properties.[7] Moreover, in MC systems, a significant population of water molecules remain tightly bound to the crowding species, thus being sequestered from bulk solvent.[8]

The cellular glycocalix (GC) is a typical example of a MC environment. The GC is a polysaccharide protective layer that conforms the environment where membrane anchored proteins are embedded.[9,10] It contributes to the antiadhesive properties of cells under normal disease free conditions and may also control the accessibility of solutes (e.g., drugs) to the cell interior and hinder the binding of targeted carriers to the cell surface.[11] The compactness of the GC is expected to affect its structure and hydration conditions. Consequently, studies on water dynamics within the molecular crowded environment of a GC would be of upmost importance to understand physical and biochemical phenomena taking place at the membrane interfacial region.

In this regard, nuclear magnetic resonance (NMR) through spin−lattice and spin−spin relaxation times has proven to be a very useful technique to provide information on aqueous solutions, on a variety of time scales and solute concentrations.[12−15] In addition, it is a noninvasive method that can be applied to a wide spectrum of solution samples. In particular, it has allowed identification of the dynamics of different water populations, helping to distinguish free liquid fractions from structured water in the presence of solutes.[16] Additionally, 1D ^{31}P NMR spectra have been extensively used to study the coexistence of different types of supramolecular aggregates (e.g., micelles and vesicles).[17,18]

Using poly(ethylene glycol) (PEG) in solution, it is possible to achieve MC conditions.[4,19,20] The ability of PEG to fulfill this role has been attributed mainly to its physical properties, such as solubility in water at all concentrations, a large exclusion volume, and a high degree of conformational entropy.[21−23] Recently, from NMR measurements of spin−lattice relaxation times of PEG^{6000} solutions, we reported the presence of two molecular populations, both in water and in PEG, as well as a PEG^{6000} aggregation also supported by dynamic light scattering

Received: November 5, 2013
Revised: May 6, 2014
Published: May 8, 2014

 © 2014 American Chemical Society dx.doi.org/10.1021/jp410894x | J. Phys. Chem. B 2014, 118, 6150−6158

data.[24] However, this model system cannot reproduce the anisotropy and molecular orientation encountered at an interface.[1−3] Thus, lipids covalently modified with hydrophilic polymers, e.g., glycolipids with both linear and branched head groups, have been considered good candidates to build up a model GC.[25,26] Additionally, lipopolymers containing poly(ethylene glycol) (PEG) have been widely used in liposome formulation for drug encapsulation and transport.[27] In these systems, PEG chains form an interfacial hydrophilic layer that prevents aggregation and nonspecific binding.[28] From both a fundamental and practical point of view, it is of interest to investigate the phase and aggregation behavior of PEG-lipid/phospholipid mixtures.[29]

In the present work, we study the water dynamics in vesicle suspensions composed of binary mixtures of dipalmitoylphosphatidylcholine (dpPC) and derivatives of dipalmitoylphosphatidylethanolamine (PE) modified with a PEG moiety: dpPC/PE−PEG^n (9:1 mol %),where n is the molar mass (350, 1000, or 5000 Da) corresponding to PEGs with 7, 23, and 113 ethylene residues, respectively (see molecular structures in Figure 1). This gave the possibility of controlling the thickness

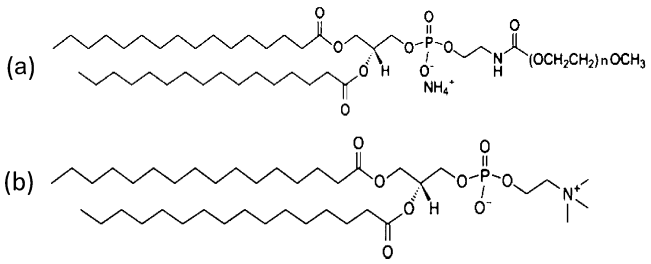

Figure 1. (a) Molecular structure of the PEG grafted phospholipid 1,2-dipalmitoyl-*sn*-glycero-3-phosphoethanolamine-*N*-[methoxy(poly(ethylene glycol))] (PE−PEG). n is the molecular mass of PE−PEG^n (350 Da (PE−PEG^{350}), 1000 Da (PE−PEG^{1000}), and 5000 Da (PE−PEG^{5000})) with 7, 23, or 113 ethylene glycol units, respectively. (b) dpPC structure (1,2-dipalmitoyl-*sn*-glycero-3-phosphoethanolamine).

of the hydrophilic interfacial region, by varying the components in the mixture. The molecular dynamics was analyzed using NMR techniques, in particular ^{1}H spin−lattice relaxation times (T_1) and ^{31}P spectra. π−MMA isotherm and compressional modulus measurements provided further structural information on these systems.

MATERIALS AND METHODS

Materials. 1,2-Dipalmitoyl-*sn*-glycero-3-phosphoethanolamine-*N*-[methoxy(poly(ethylene glycol))] with PEG average molecular masses of 350, 1000, and 5000 (PE−PEG^{350}, PE−PEG^{1000}, PE−PEG^{5000}, respectively) and 1,2-dipalmitoyl-*sn*-glycero-3-phosphocholine (dpPC) were purchased from Avanti Polar Lipids (Alabaster, AL), DiI-C$_{18}$, 1,1′-dioctadecyl-3,3,3′,3′-tetramethylindocarbocyanine perchlorate was from Molecular Probes Inc. (Eugene, OR), and virgin deuterated water was kindly donated by Central Nuclear Embalse de Río Tercero, Córdoba, Argentina.

Methods. *Membrane Preparation.* Figure 1 displays the dpPC/PE−PEG^n systems for n = 350, 1000, and 5000 prepared as follows. Stock solutions of the pure compounds were mixed in the appropriate proportion (dpPC:dpPE−PEG (9:1) molar ratio) in chloroform:methanol (2:1); then, the solvent was evaporated under a nitrogen stream. In a previous work, through the Langmuir film balance technique, we studied the mixing behavior of dpPC/PE−PEG^n finding that the thin films containing PE−PEG^{1000} or PE−PEG^{5000} formed stable monolayers in mixtures with dpPC up to a lipopolymer molar fraction of x = 0.2, and up to x = 0.1 in the case of PE−PEG^{350}.[30]

The film thus formed was left under a vacuum for no less than 2 h to remove residual solvent. Lipids were resuspended to reach 20 mM concentration in deuterated water at 50 °C, by 3 min of vortexing to form multilamellar vesicles (MLVs). The MLV suspension was tip sonicated for 45 min using a SonaBox Ultrasonic Homogenizer 150 VT (Biologics Inc., Manassas, VA) to obtain small unilamellar vesicles (SUVs). Alternating cycles of sonication and rest (30 s) were made in an ice water bath to keep the temperature between 0 and 4 °C. Samples were then centrifuged at 10 000g for about 20 min to remove any residual large particles and titanium released from the sonicator tip. The SUVs were used in all ^{1}H NMR and ^{31}P NMR experiments.

NMR Experiments. ^{1}H spin−lattice relaxation times (T_1) were measured for all the systems in a Bruker Avance 400 MHz spectrometer using the inversion−recovery (IR) pulse sequence (π-*t*-π/2-*Acquisition*).[31] Liposomes were dispersed in D_2O containing trace amounts of H_2O. Then, separated resonances belonging to the ^{1}H nucleus in phospholipids, the PEG moiety from lipopolymers, and H_2O were observed, enabling the spectral resolution of proton signals belonging to different parts of the system. The recovery times in the IR experiments t ranged between 10 μs and 128 s.

^{31}P NMR spectra for all the systems were measured at 121.49 MHz ^{31}P frequency on a Bruker Avance 300 MHz spectrometer. These spectra were obtained performing a π/2 pulse of 9.4 μs with ^{1}H decoupling during acquisition with a proton field of 60 kHz. The recycling time was 4 s, and 6000 scans were accumulated for each sample.

All the NMR experiments were performed at 37 °C in order to emulate the biological conditions.

π−MMA Isotherm Recording. Surface pressure−mean molecular area compression isotherms were obtained for pure or mixed lipid monolayers as described before at different surface pressures.[32] Briefly, experiments were performed at 37 ± 1 °C, with a Minitrough II (KSV Instruments Ltd., Finland) enclosed in an acrylic box to avoid surface contamination, which measured the surface pressure (π) with the Wilhelmy plate method. The absence of surface-active compounds in the pure solvents and in the subphase solution was routinely checked before each run by reducing the available surface area to less than 10% of its original value, after allowing enough time for the adsorption of possible impurities that might have been present in trace amounts.

The lipid mixture was dissolved in chloroform−methanol (2:1 V/V) and spread on the air−water surface. After the solvent evaporation and the monolayer stabilization, the interface was compressed at a constant rate of 10 mm/min. A lower compression rate (1 mm·min^{-1}) was tested with identical results. π and molecular area (A) were registered during the process with a precision within ±1 mN/m and ±0.01 nm^2, respectively. From the π−A isotherms, the surface parameters, minimum molecular area, A_{min}, and collapse pressure, π_c, were obtained. A_{min} is the minimum area occupied by an amphipathic molecule in a monolayer at the closest molecular packing, and the collapse pressure π_c is the maximal π that corresponds to A_{min}. The latter parameter is related to monolayer stability and can be associated with intermolecular

dx.doi.org/10.1021/jp410894x | J. Phys. Chem. B 2014, 118, 6150−6158

cohesion forces of the amphipathic molecules, the affinity of the polar groups for the aqueous subphase, and the optimal hydrophobic−hydrophilic balance in the molecule.

Isotherms shown in Figure 6 are typical examples with high overall reproducibility (e.g., errors in area measurements ranged between 3 and 5%).

Compressional Modulus. The compressional modulus K was calculated for each isotherm according to eq 2:

$$K = -(A_\pi)\cdot\left(\frac{\delta\pi}{\delta A}\right)_T \quad (1)$$

where A is the mean molecular area (MMA). K allows inferring about the elasticity of the monolayer, and to define more precisely the bidimensional phase transitions from the π−MMA isotherm profile.

For ideal mixtures with a defined composition, an ideal K (K_{id}) was calculated as the weighted sum of the reciprocals of the compressibilities for individual monolayer components ($1/C_i$) using the molar fraction (x_i) as the weighting factor, according to eqs 2 and 3.

$$K_{id} = \sum x_i \cdot \frac{1}{C_i} \quad (2)$$

$$C_i = -\left(\frac{1}{A_i}\right)\cdot\left(\frac{\delta A_i}{\delta\pi}\right)_T \quad (3)$$

Epifluorescence Microscopy. Epifluorescence microscopy (EFM) was performed as described previously.[33] Pure lipid monolayers were doped with 1−2 mol % of DiI-C_{18} and observed with an inverted epifluorescence microscope directly from the interface. Briefly, a KSV Minisystem surface barostat was mounted on the stage of a Nikon Eclipse TE2000-U (Tokyo, Japan) microscope, which was supplied with 209 extra large working distance optics. The Teflon trough used had a 35 mm diameter quartz window at its base, which allowed the observation of the monolayer through the trough. The monolayer morphology was documented with a Nikon DS-5 M color video camera with a supported resolution up to 2560−1920 pix (Capture).

Dynamic Light Scattering (DLS). An aqueous dispersion of dpPC/PE−PEG^n (9:1) with n = 350, 1000, and 5000 was introduced into the thermostatized sample cell of a Nicomp Model 380 Submicrometer Particle Sizer (PSS, CA, USA), using a 632.8 nm laser source at a fixed scattering angle of 90°. Each sample was measured at least twice for 10 min. The solvent (distilled D_2O) was filtrated through regenerated cellulose Amicom Ultra (Millipore, Billerica, MA, USA) filters with 10 000 MWCO to eliminate contaminant particles. Data were collected and analyzed with the software provided with the instrument, which utilizes the NICOMP algorithm for diameter calculations. The channel width was automatically set by the instrument, and the refraction index and viscosity of the solvent were obtained from the literature.

RESULTS AND DISCUSSION

The general structure of the three PE−PEG^n used is summarized in Figure 1.

PE−PEG^{350} is the smallest of the three biopolymers analyzed, with a molecular weight (MW) of 1075.4 Da. From the three PE−PEG derivatives studied, PE−PEG^{350} is the most similar to a phospholipid and has the least significant contribution to the molecular density (crowding) of the hydrophilic layer formed by the PEG moiety at the interfacial region of mixed vesicles. In the case of PE−PEG^{1000} (MW = 1736.18 Da), the volume ratio between the polar headgroup (PH) and the hydrophobic hydrocarbon chain (HC) regions is quite balanced, providing a higher molecular density in the hydrophilic layer formed by PEG with some extension parallel to the membrane normal. PE−PEG^{5000} is the most massive lipopolymer used in this study (MW = 5745 Da). The high ratio between the size of its PH and the HC suggests a detergent-like behavior.[34] However, contrary to what would be expected, the pure compound is able to form stable monolayers at the air−water interface.[35] Here it is also stabilized in the mixture with dpPC. The big size of the PEG moiety in this molecule precludes a high molecular density in the hydrophilic layer.

^{1}H NMR. The ^{1}H NMR spectra for dpPC/PE−PEG^n systems are depicted in Figure 2.

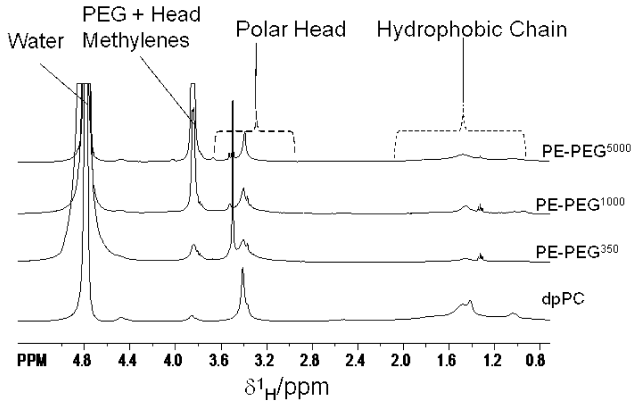

Figure 2. ^{1}H NMR spectra of D_2O dispersions of dpPC/PE−PEG^n with n = 50, 1000, or 5000. Proton signals have been divided into four regions for better comprehension and to perform the integrals in the inversion−recovery experiments: the signal of residual water at 4.8 ppm, the polar head (PH) of dpPC, the hydrophobic tail (HC) of dpPC, and the PEG region overlapped with the head methylenes.

There, we show the assignment of ^{1}H signals coming from phospholipid and lipopolymer moieties named HC (within 0.8−1.9 ppm), PH (in the region 3.2−3.6 ppm), and PEG (at 3.8 ppm), together with the signal at 4.8 ppm corresponding to H_2O, which was present in trace amounts. In the inversion−recovery experiments, each region was integrated separately to obtain the normalized ^{1}H magnetization, $M(t)$, as a function of t. These $M_X(t)$ curves followed a biexponential behavior

$$M_X(t) = M_0(1 - 2A\exp(-t/T_{1A}) - 2(1 - A)\exp(-t/T_{1B})) \quad (4)$$

where X stands for HC, PH, PEG, and H_2O. The parameters A and $(1 - A)$ can be directly interpreted as the proportions of each T_1 population sample. In the case A = 1, the fitted function resulted in being monoexponential, exhibiting only one relaxation time. Figure 3 displays the experimental data of $\ln(1 - M_X(t)/M_0)$ and the corresponding fittings of eq 4, for the dpPC/PE−PEG^{1000} mixture.

In all of the species and molecular moieties analyzed, our results showed the presence of two ^{1}H populations with long (T_{1A}) and short (T_{1B}) relaxation times, respectively. Table 1 summarizes the relaxation times T_{1A} and T_{1B}, and Table 2

dx.doi.org/10.1021/jp410894x | J. Phys. Chem. B 2014, 118, 6150−6158

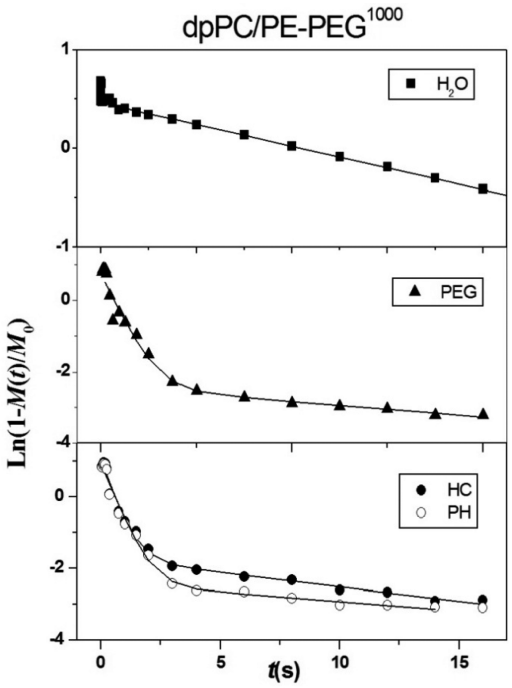

Figure 3. ^{1}H magnetization data of the inversion−recovery experiment as a function of time, $\ln(1 - M(t)/M_0)$, and the corresponding fittings to eq (4) for mixed dpPC/PE−PEG^{1000} vesicles. M_{H_2O} is shown at the top, M_{PEG} is shown in the middle, and M_{HC} and M_{PH} are shown together at the bottom.

summarizes the proportion of ^{1}H-T_{1B} population in each chemical species or residue analyzed (P^B).

Table 1. ^{1}H-T_1 Values (T_{1A} and T_{1B}) Obtained from Two-Exponential Fittings Performed to $M(t)$ of the Inversion−Recovery Experiments for the Systems dpPC/PE−PEG^n, for All the Regions Resolved in ^{1}H Spectra

	^{1}H-T_1 (s)					
	dpPC/PE−PEG^{350}		dpPC/PE−PEG^{1000}		dpPC/PE−PEG^{5000}	
chemical group	T_{1A}	T_{1B}	T_{1A}	T_{1B}	T_{1A}	T_{1B}
H_2O	16.8	0.22	18.1	0.19	20	0,03
HC	9.5	0.24	13	0.53	19	0.67
PH	8.4	0.29	17	0.63	19	0.66
PEG	33	0.26	20	0.68		0.86

Table 2. ^{1}H Proportions Associated to T_{1B} for All the Regions Resolved in the ^{1}H Spectra for the Systems dpPC/PE−PEG^n, Obtained from Two-Exponential Fittings Performed to $M(t)$ in the Inversion−Recovery Experiments

	P^B (proportion of T_{1B})		
chemical group	dpPC/PE−PEG^{350}	dpPC/PE−PEG^{1000}	dpPC/PE−PEG^{5000}
H_2O	0.26	0.17	0.12
HC	0.92	0.92	0.95
PH	0.92	0.94	0.95
PEG	1	0.93	1

In our system, long relaxation times were in the order of 16.8−20 s for water, around 20−30 s for PEG, and in the range 8−19 s for PH and HC. In contrast, short relaxation times were found in the range 0.03−0.22 s for water, while for PEG, PH, and HC, the values were between 0.24 and 0.86 s (Table 1). A T_1 of 22 s corresponding to pure water has been measured previously.[24]

Figure 4 is a comparative plot of the long and short relaxation times (T_{1A} and T_{1B}) for the different components

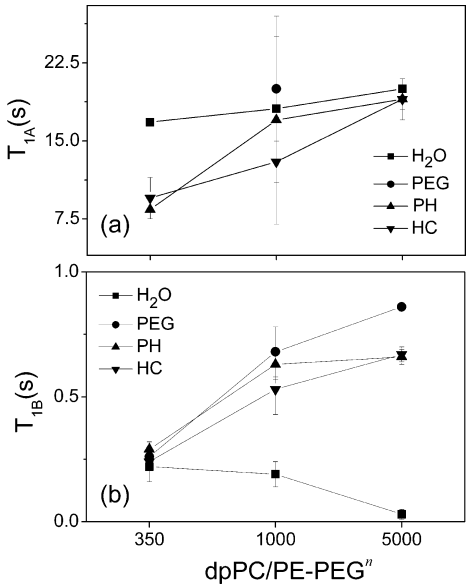

Figure 4. Long and short relaxation time values in PEGylated phospholipids, as a function of PEG chain length, n, obtained by fitting a two-exponential function to the magnetization ($M_X(t)$), where X is H_2O, PEG, HC, or PH: (a) long relaxation times, T_{1A}; (b) short relaxation times, T_{1B}.

involved in the mixture. Note that the larger fitting errors for T_1 values always appear in the case of the component with the smallest proportion, that is, B component in water and A component for the solid parts (PEG, HC, PH) (see Table 2).

Longitudinal (spin−lattice) relaxation times are related to the correlation times associated with a particular motion. T_1 is also dependent on the Larmor frequency (in our case, 400 MHz) and the strength of the interactions of the local fields.[31] In particular, in the extreme narrowing condition valid for mobile solutions, T_1 is inversely proportional to the motional correlation times. In that limit, T_1 values are decreasing when the fluctuation correlation time increases (i.e., more viscous solutions), while far from this condition T_1 increases with the fluctuation correlation time.[31]

T_{1A} of water is associated with the faster dynamics, while T_{1B} of water is related to slower molecular motion. We can see from Figure 4 and Table 1 that T_{1A} values for water increase with n. Taking into account the mentioned dependence of T_1 with correlation times for mobile solutions, this behavior is indicative of a decreasing viscosity and faster molecular mobility of water in suspensions containing lipopolymers with longer PEG moieties. ^{31}P NMR 1D spectra provided a hypothesis to explain this behavior (see below). In contrast, T_{1B} values corresponding to water showed a decreasing tendency as a function of the size of the PEG moiety, reflecting a motion restriction which grows with n and may be ascribed to confined water molecules. Interestingly, the proportion P^B of immobilized water decreases with n (Table 2). This may be explained by a reduction in the size of the compartment containing the pool of confined water.

dx.doi.org/10.1021/jp410894x | J. Phys. Chem. B 2014, 118, 6150−6158

Upon comparing T_{1A} values for PH and HC moieties in the three PE−PEG^n, a slight increase with n (Figure 4a) can be observed with values remaining similar between one another if considered within the same lipopolymer. The latter indicates that the phospholipid components in a lipopolymer are strongly connected and belong to the same proton system. T_{1A} components for PEG moieties with n = 350 and 1000 have values significantly higher than those of HC and PH in the same compound and followed the opposite tendency decreasing with n. This suggests that the PEG moiety behaves almost independently with respect to the phospholipid part of the lipopolymer. In PE−PEG^{5000}, it was not possible to resolve a biexponential behavior for PEG. It is important to note that T_{1A} for PEG, PH, and HC exhibited the lowest contribution to the total spin−lattice relaxation time (P^A) (Table 2).

The short relaxation time, T_{1B}, is the component of the spin−lattice relaxation time most populated ($P^B > P^A$) in PEG as well as in PC and PH residues in phospholipids (Table 2). T_{1B} values for the less mobile components (PEG, PH, and HC) follow the same increasing tendency with n. This is indicative of a widening in fluctuations within phospholipids and PE−PEG^n molecules in the self-aggregating structures containing lipopolymers. The increase in n can be associated with molecules with a more pronounced cone shape and a stronger tendency to self-aggregate in structures of higher surface curvature and lower molecular packing. This is a consequence of geometrical constraints and steric restrictions that lead to packing tensions. The latter are relieved through a decrease in particle size and an increase in surface curvature up to the point of changing the type of self-assembly (from bilayer to micelle) (see below ^{31}P NMR data). The smallest structures are expected to have the lowest molecular packing, mainly within the outer leaflet in bilayers.[36] In PE−PEG^{350}, T_{1B} values for all of the components (PEG, PH, and HC) are around 0.24−0.29 s. This behavior is probably due to the strong connections in the PE−PEG^{350} system that behaves very similar to dpPC creating a homogeneous environment. On the contrary, for n = 5000, the T_{1B} value in PEG (0.86 s) differs from those of HC (0.67 s) and PH (0.66 s).

Recently, from NMR measurements of spin−lattice relaxation times (T_1) in PEG^{6000} water solutions, we reported the presence of two molecular populations, both in water and in PEG, as well as a PEG^{6000} aggregation also supported by dynamic light scattering data.[24] In the present work, the existence of two dynamical contributions to the system could be explained either by an equilibrium between two molecular conformations (phase coexistence) or by the presence of different types of supramolecular aggregates. The transition between liposomes and micelles as a function of PEG size and concentration with the apparition of disk-like micelles and coexistence of liposomes and micelles have been studied recently.[29,37]

In order to explore both possibilities explained above, we first performed ^{31}P NMR spectra and DLS experiments in aqueous suspensions, and π−MMA compression isotherms and EFM experiments in Langmuir films for all of the systems.

^{31}P NMR. ^{31}P NMR is a powerful technique to explore biomembranes and model systems. Performing ^{1}H decoupling, the ^{31}P spectrum is mainly affected by the chemical shift anisotropy (CSA). In the hypothetical case of motionless, randomly oriented membrane structures, the ^{31}P spectrum corresponds to a powder pattern generated by adding up spectra for all possible orientations (inhomogeneous line). In the opposite case, in micelles, the rapid reorientation in the NMR time scale produces a total average of the anisotropies yielding a narrow signal, like in the case of nonviscous solutions with isotropic motion. In the case of lamellar liposomes and cylindrical structures, the spectrum exhibits a characteristic powder pattern shape with a peak and a shoulder. Then, ^{31}P NMR can be used to distinguish between micelles and liposome aggregates, which relies on the fact that a bigger entity (liposome) produces a wider signal than a smaller micellar particle.[17,38] In liposomes, the chemical shift anisotropy (CSA) is measured as the width between the low field shoulder and the main high field peak of the anisotropic spectrum, reflecting the orientation of the phosphate groups in the bilayer.[17,38,39] The CSA value depends on the molecular and intramolecular motional averaging.

Figure 5 shows the one-dimensional (1D) ^{31}P NMR spectra for all of the systems under study. For dpPC/PE−PEG^{350,1000}, a typical shoulder for a bilayer structure is observed, where the CSA is 20 ppm (2400 Hz) for n = 350 and 13 ppm (1600 Hz) for n = 1000. The smaller value of CSA for n = 1000 reflects a stronger motional averaging in comparison with n = 350. In contrast, for dpPC/PE−PEG^{5000}, the phosphate shows a quite symmetric peak associated with a more isotropic motion, indicating the prevailing presence of micelles. These spectra allowed us to discard the coexistence of different types of supramolecular aggregates. The formation of liposomes and micelles is related to the PEG chain length. Then, for n = 350 and 1000, the inclusion of PEG confers a cylindrical geometry to the macromolecule favoring the formation of bilayers, while, for n = 5000, the long chain of PEG and the big size of the polar headgroup leads to a conical molecular geometry inducing the formation of micelles.[34,40] Then, in all cases, the ^{31}P 1D spectra lead to the conclusion that only one kind of particles is present (micelles or vesicles).

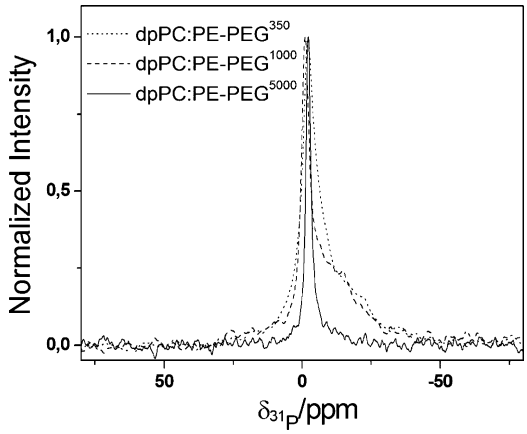

Figure 5. ^{31}P NMR spectra of mixed vesicles composed of dpPC and 10 mol % PE−PEG^n, where n = 350, 1000, or 5000, dispersed in D_2O.

Assuming a smaller size for micelles compared with bilayer vesicles, a lower viscosity may be expected for dispersions of particles containing PE−PEG^{5000} (micelles) with respect to those containing PEGs with n = 350 and 1000 (bilayer vesicles). Note that viscosity has been proven to decrease upon lowering the size of the nanoparticles in dispersions above a concentration threshold.[41] Thus, higher n would correlate with lower particle size (Figure 5) and lower viscosity[41] and would

dx.doi.org/10.1021/jp410894x | J. Phys. Chem. B 2014, 118, 6150−6158

explain the increase in T_{1A} for water as a function of n (Figure 4a).

Phase transitions within the polymer regions and phase coexistence within the membrane plane may explain the different T_1 components found in PH, PC, and PEG moieties in lipidic molecules.

EFM and π–MMA Isotherm. In order to gain further insight into the behavior of the dpPC/PE–PEG^n mixtures, an analysis of π–A isotherms is included. Moreover, EFM on Langmuir monolayers of the mixtures was performed. The π–MMA isotherms, at 37 ± 1 °C, from the 9:1 mixtures of dpPC with PE–PEG^n with n = 350, 1000, and 5000 are shown in Figure 6.

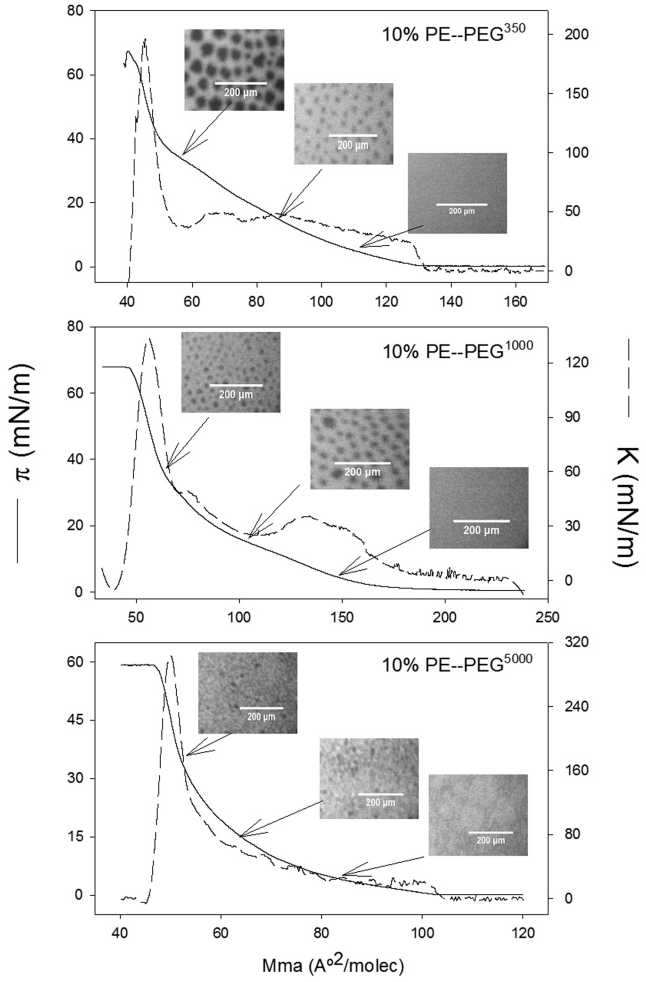

Figure 6. π–A isotherms for 9:1 binary mixtures of dpPC/PE–PEG^n, with n = 350 (a), 1000 (b), or 5000 (c), respectively. Compressibility modulus (dashed lines) for each compression isotherm, and accompanied by three epifluorescence micrographs at different lateral pressures of 5, 15, and 35 mN/m.

The mixtures containing PE–PEG^{350} and PE–PEG^{1000} exhibit a smooth shape in their π–MMA and K–MMA isotherms which is in accordance with the homogeneous aspect of the EFM images at 5 mN/m. Upon an increase in the lateral pressure, two transitions referred to as t1 and t2 appear in Figure 6. They correlate with minima in K–MMA isotherms and with the presence of condensed domains at the interface exhibited by the EFM images. While t1 becomes completed at ∼19 and 15 mN/m for PE–PEG^{350} and PE–PEG^{1000}, respectively, t2 is observed at higher π (at 33 and 30 mN/m, respectively) (Figure 6a and b). In the film containing PE–PEG^{5000}, the whole π–MMA isotherm looks smooth until the collapse pressure at 58 mN/m. Neither the compressional modulus detects a slope change in the π–MMA isotherm nor the EFM exhibits condensed domains typically due to phase coexistence. However, the rough image may reflect molecular aggregates fixed at the interface coming from a partial collapse of the monolayer (Figure 6c). At 58–60 mN/m, the collapse of all monolayers was at a surface pressure compatible with the collapse of an excess of pure dpPC.

To understand these results, it is important to recall that the π–A isotherms of pure dpPC at 30–40 °C exhibit a 2D transition at $\pi \sim$ 20–30 mN/m characteristic of the liquid expanded–liquid condensed 2D phase transition.[42,43] On the other hand, pure PE–PEG^n lipopolymers with $n \geq 1000$ at a low molecular packing have been shown to have their polymeric tails lying at the air–water interface (pancake conformation) which desorbs from the interface at $\pi \sim 6$ mN/m acquiring a random coil conformation (mushroom). At ∼30 mN/m, lipopolymers with $n \leq 1000$ suffer another conformational transition within the polymeric tails toward a stretched conformation (brush), which is driven and stabilized by interactions within the hydrocarbon chains.[44,45] Both conformations can be achieved by PEGylated lipopolymers, within certain compositional ranges, in mixed liposomes containing other phospholipids.[46] The mushroom–brush transition has been shown to occur at a 0.22 PE–PEG^{350} molar fraction and at a 0.03 molar fraction of PE–PEG^{5000} in mixtures containing these lipopolymers.

Taking this information together, it can be concluded that the mixed monolayers of dpPC and PE–PEG^n do not show the pancake–mushroom transition (Figure 6). While t1 in lipopolymers with n = 350 and 1000 can be ascribed to a 2D phase transition within segregated dpPC, t2 may be associated with a mushroom–brush transition within the polymeric tails of PE–PEG^{350,1000}. The absence of a 2D phase transition in the mixture containing PE–PEG^{5000} indicates the mixed condition of the components at low lateral pressure and an impairment of the hydrocarbon chain condensation due to a steric hindrance imposed by the bulky polymeric moiety.

The actual PC/PE–PEG^n molar ratio in the monolayers is expected to be the same as that of the initial solution spread over the air–water interface. However, a destabilization phenomenon might be induced at high lateral compression (higher π) and high temperatures, leading to a loss of monolayer components and possibly a change in the molecular composition of the interface. Moreover, the lift-off area (LOA) should increase with the molecular weight of PEG. This behavior was followed up in mixtures containing PE–PEG^{350} to PE–PEG^{5000} at 25 °C (not shown), but at 37 °C (present work), the LOA of dpPC/PE–PEG^n followed the sequence 130, 170, and 120 Å^2/mol for n = 350, 1000, and 5000. The breaking of the upward tendency in the value of LOF suggests a particular unstable behavior and the loss of monolayer in samples containing PEG^{5000} (Figure 7c). Then, the increase in temperature may be the main contributor to the loss of area in this sample. At present, we are not able to evaluate the final monolayer composition. However, it is interesting to note that the behavior of dpPC/PE–PEG^{5000} in the monolayer phase reflects the tendency of molecules to escape from the planar organization which is consistent with molecules in aqueous

dx.doi.org/10.1021/jp410894x | J. Phys. Chem. B 2014, 118, 6150–6158

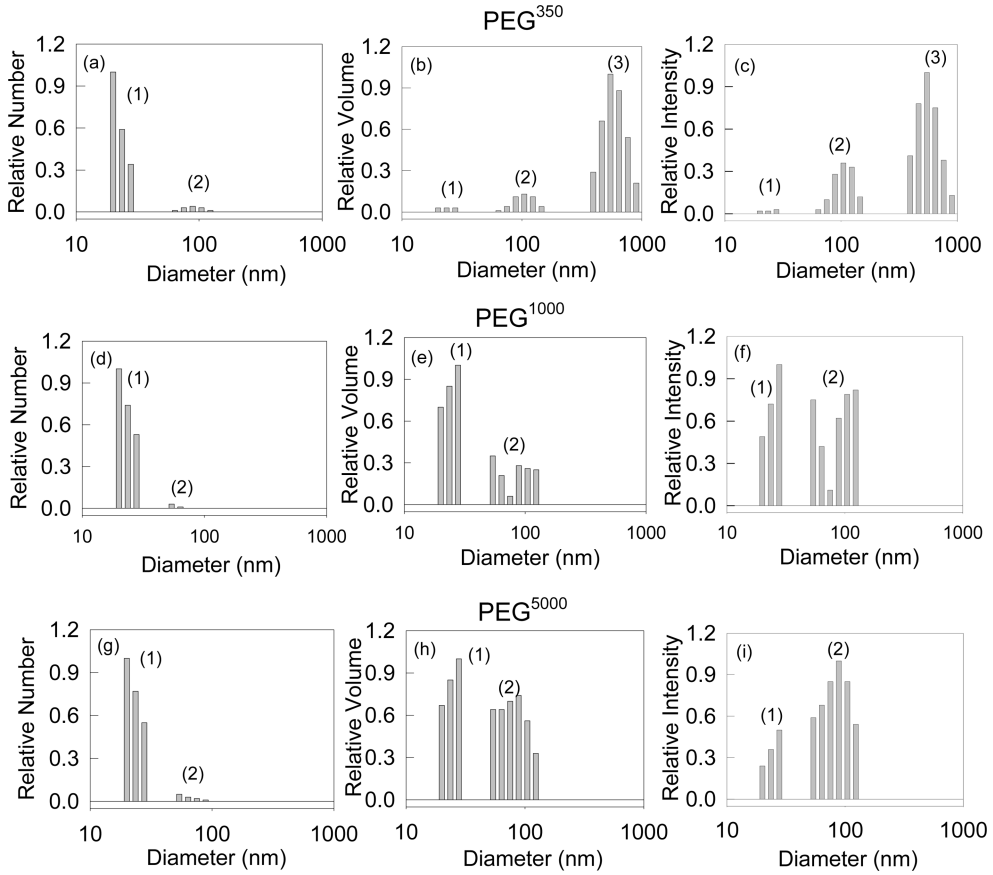

Figure 7. DLS analysis, by number (a, d, g), by volume (b, e, h), and by intensity (c, f, i) of 9:1 binary mixtures of dpPC/PE−PEG^n, with n = 350 (a, b, c), 1000 (d, e, f), or 5000 (g, h, i), respectively. Three peaks (1, 2, 3) were identified according to their diameter size. Note that intensity should be the less affected by the "degree of ill-conditioning" in the inversion of the Laplace transform of measured data.[48]

suspension preferring to form self-aggregating structures with high curvature (micelle), as shown by ^{31}P NMR data.

DLS. A DLS analysis of all dispersions was performed, and particle size distribution was analyzed by number, by volume, and by intensity. Results are depicted in Figure 7.

In samples containing PEG^{350}, we found three peaks (identified as 1, 2, and 3) corresponding to particles with average diameters within 25 (20−30) nm, 90 (60−120) nm, and 600 (400−900) nm, respectively. Peak 1 was significantly more abundant than the other two peaks. Peak 3 was represented by a very small amount of big particles, as indicated by the fact that it could only be detected through the analysis by volume and not by number. According to the order of magnitude of the average diameters found, it can be suggested that peaks 1 and 2 might be due to small (SUVs) and large unilamellar vesicles (LUVs) and peak 3 to multilamellar vesicles (MLVs). The latter is consistent with data obtained through SAXS and TEM experiments with aqueous dispersions of HSPC/PEG400 mixtures.[47]

In dpPC/PEG^{1000} and dpPC/PEG^{5000} samples, only peaks 1 and 2 could be identified. In these samples, the contribution of peak 2 to the relative volume was more significant than in dpPC/PEG^{350} samples. According to ^{31}P NMR data, peak 1 in dpPC/PEG^{5000} samples in the present work is expected to be due to micellar particles exhibiting a size smaller than that reported in the literature for disk-like micelles present in nonsonicated dpPC/8.3 mol % PE−PEG^{5000} samples.[29] Peak 2 in dpPC/PEG^{5000} may include structures containing a bilayer phase (bicelles or vesicles) in a very small proportion that justifies the slight asymmetry of the ^{31}P spectrum recorded in this sample.

CONCLUSIONS

In this work, we have studied molecular crowded systems modeled by suspensions of binary mixes (9:1) of dpPC and PE modified with PEG having different chain sizes. Performing ^{1}H NMR spin−lattice relaxation time measurements with spectral resolution, we could distinguish two ^{1}H populations in each component of the solute (PEG and phospholipids) and the solvent (water), having very different T_1 values, leading to the possibility of phase coexistence (micelles with liposomes) or different interfacial domains. The tendency of the T_1 values leads to the conclusion that the solvent decreases its viscosity and the aggregates reduce its size as a function of the PEG chain size.

$T_{1B}^{H_2O}$ reports the behavior of the most immobilized water molecules, mainly those confined in the aqueous compartment of vesicles—also occupied by motion restricted PEG chains—becomes less abundant (lower $P_{1B}^{H_2O}$) according to the particle size decreases or the particle type changes from vesicle to micelle. In turn, $T_{1A}^{H_2O}$, the most populated of both $T_1^{H_2O}$ components, would report the behavior of structured water (molecules tightly bound to disordered PEG) plus bulk water which is the dispersing media of self-assembling lipid particles. The dispersion viscosity is expected to decrease with the decreasing size of dispersed particles. This would over-compensate the increase in the amount of PEG^n-bound water and explains the increasing $T_{1A}^{H_2O}$ values as a function of n.

dx.doi.org/10.1021/jp410894x | J. Phys. Chem. B 2014, 118, 6150−6158

T_{1A} for HC, PH, and PEG exhibited low probability (in the case of PEG^{5000}, it was almost zero), and the tendency followed was $T_{1A}^{HC} \sim T_{1A}^{PH} < T_{1A}^{PEG}$. T_{1B} for PEG and for the lipidic regions HC and PH is the most populated of both T_1 for these molecular regions, behaves as a common proton system, and increases with n, although T_{1B}^{PEG} seems to grow faster.

The measurements of ^{31}P spectra led to the conclusion that for n = 350 and 1000 there are liposomes with reduced size and for n = 5000 there are almost only micelles. The distinguishing behavior in ^1H NMR populations present in PEG, PH, and HC regions of phospholipid and lipopolymer molecules in conjunction with ^{31}P NMR spectra allowed us to postulate that they corresponded to the different domains in a bilayer phase in samples containing lipopolymers with n = 350 and 1000. The presence of these domains was confirmed by EFM in monolayers at around 30 mN/m, which is the expected surface pressure present in bilayers.[49] In the case of dpPC/PEG^{5000}, both T_1's observed for PH and HC moieties might be represented by different types of self-aggregated structures.

All of these experiments confirmed the sensitivity of the NMR technique to study macromolecular crowded media not only for giving information about water dynamics but also for giving information about the different aggregate phases and conformations.

AUTHOR INFORMATION

Corresponding Author

*E-mail: mperillo@efn.uncor.edu. Fax: +54-351-4334139.

Notes

The authors declare no competing financial interest.

ACKNOWLEDGMENTS

The authors are members of the Research career of the Consejo Nacional de Investigaciones Científicas y Técnicas (CONICET) from Argentina. The present work was supported by grants from Foncyt, CONICET, and SeCyT-Universidad Nacional de Córdoba.

ABBREVIATIONS

FID, free induction decay; NMR, nuclear magnetic resonance; PEG, poly(ethylene glycol); [PEG], poly(ethylene glycol) concentration; GC, glycocalix; dpPC, dipalmitoylphosphatidylcholine; HC, hydrocarbon chain; ^1H, proton; MLVs, multilamellar vesicles; PE, dipalmitoylphosphatidylethanolamine; PH, polar head; T_1, spin−lattice relaxation time; T_{1A}^X, T_{1B}^X, long and short relaxation time components in the X peak (Bruker 400 MHz experiment) (where X = PEG, H_2O, HC, or PH)

REFERENCES

(1) Fulton, A. B. How Crowded Is the Cytoplasm? *Cell* **1982**, *30*, 345−347.
(2) Ellis, R. J.; Minton, A. P. Cell Biology: Join the Crowd. *Nature* **2003**, *425*, 27−28.
(3) Zimmerman, S. B.; Trach, S. O. Estimation of Macromolecule Concentrations and Excluded Volume Effects for the Cytoplasm of Escherichia Coli. *J. Mol. Biol.* **1991**, *222*, 599−620.
(4) Chebotareva, N. A.; Kurganov, B. I.; Livanova, N. B. Biochemical Effects of Molecular Crowding. *Biochemistry (Moscow)* **2004**, *69*, 1239−1251.
(5) Ellis, R. J. Macromolecular Crowding: Obvious but Underappreciated. *Trends Biochem. Sci.* **2001**, *26*, 597−604.
(6) Ellis, R. J. Macromolecular Crowding: An Important but Neglected Aspect of the Intracellular Environment. *Curr. Opin. Struct. Biol.* **2001**, *11*, 114−119.
(7) Hall, D.; Minton, A. P. Macromolecular Crowding: Qualitative and Semiquantitative Successes, Quantitative Challenges. *Biochim. Biophys. Acta* **2003**, *1649*, 127−139.
(8) Ellis, R. J.; Minton, A. P. Protein Aggregation in Crowded Environments. *Biol. Chem.* **2006**, *387*, 485−497.
(9) Clop, E. M.; Perillo, M. A. Langmuir Films from Human Placental Membranes: Preparation, Rheology, Transfer to Alkylated Glasses, and Sigmoidal Kinetics of Alkaline Phosphatase in the Resultant Langmuir-Blodgett Film. *Cell Biochem. Biophys.* **2010**, *56*, 91−107.
(10) Huang, T. M.; Hung, H. C.; Chang, T. C.; Chang, G. G. Solvent Kinetic Isotope Effects of Human Placental Alkaline Phosphatase in Reverse Micelles. *Biochem. J.* **1998**, *330* (Pt 1), 267−275.
(11) Gouverneur, M.; Berg, B.; Nieuwdorp, M.; Stroes, E.; Vink, H. Vasculoprotective Properties of the Endothelial Glycocalyx: Effects of Fluid Shear Stress. *J. Intern. Med.* **2006**, *259*, 393−400.
(12) Vackier, M.-C.; Hills, B. P.; Rutledge, D. N. An NMR Relaxation Study of the State of Water in Gelatin Gels. *J. Magn. Reson.* **1999**, *138*, 36−42.
(13) Sabadini, E.; Egidio, F. d. C.; Fujiwara, F. Y.; Cosgrove, T. Use of Water Spin-Spin Relaxation Rate to Probe the Solvation of Cyclodextrins in Aqueous Solutions. *J. Phys. Chem. B* **2008**, *112*, 3328−3332.
(14) Kuentz, M.; Rothenhäusler, B.; Röthlisberger, D. Time Domain ^1H NMR as a New Method to Monitor Softening of Gelatin and Hpmc Capsule Shells. *Drug Dev. Ind. Pharm.* **2006**, *32*, 1165−1173.
(15) Demangeat, J.-L. NMR Water Proton Relaxation in Unheated and Heated Ultrahigh Aqueous Dilutions of Histamine: Evidence for an Air-Dependent Supramolecular Organization of Water. *J. Mol. Liq.* **2009**, *144*, 32−39.
(16) Wilkinson, D. A.; Morowitz, H. J.; Prestegard, J. H. Hydration of Phosphatidylocholine. Adsorption Isotherm and Proton Nuclear Magnetic Resonance Studies. *Biophys. J.* **1977**, *20*, 169−179.
(17) Leal, C. l.; RÃ¶gnvaldsson, S.; Fossheim, S.; Nilssen, E. A.; Topgaard, D. Dynamic and Structural Aspects of Pegylated Liposomes Monitored by NMR. *J. Colloid Interface Sci.* **2008**, *325*, 485−493.
(18) Triba, M. N.; Warschawski, D. E.; Devaux, P. F. Reinvestigation by Phosphorus NMR of Lipid Distribution in Bicelles. *Biophys. J.* **2005**, *88*, 1887−1901.
(19) Farruggia, B.; Nerli, B.; Pico, G. Study of the Serum Albumin-Polyethyleneglycol Interaction to Predict the Protein Partitioning in Aqueous Two-Phase Systems. *J. Chromatogr. B: Anal. Technol. Biomed. Life Sci.* **2003**, *798*, 25−33.
(20) Pico, G.; Romanini, D.; Nerli, B.; Farruggia, B. Polyethyleneglycol Molecular Mass and Polydispersivity Effect on Protein Partitioning in Aqueous Two-Phase Systems. *J. Chromatogr. B: Anal. Technol. Biomed. Life Sci.* **2006**, *830*, 286−292.
(21) Elbert, D. L.; Hubbell, J. A. Surface Treatments of Polymers for Biocompatibility. *Annu. Rev. Mater. Sci.* **1996**, *26*, 365−294.
(22) de Gennes, P. G. Conformations of Polymers Attached to an Interface. *Macromolecules* **1980**, *13*, 1069−1075.
(23) Lee, J. H.; Lee, H. B.; Andrade, J. D. Blood Compatibility of Polyethylene Oxide Surfaces. *Prog. Polym. Sci.* **1995**, *20*, 1043−1079.
(24) Clop, E. M.; Perillo, M. A.; Chattah, A. K. ^1H and ^2H NMR Spin-Lattice Relaxation Probing Water: Peg Molecular Dynamics in Solution. *J. Phys. Chem. B* **2012**, *116*, 11953−11958.
(25) Schneider, M. F. Forces, Thermodynamics and Structure of Artificial Glycocalyx Models in Two and Three Dimensions. Technische Universitat, Munchen, 2003.
(26) Schneider, M. F.; Lim, K.; Fuller, G. G.; Tanaka, M. Rheology of Glycocalix Model at Air/Water Interface. *Phys. Chem. Chem. Phys.* **2002**, *4*, 1949−1952.
(27) Kim, J. Y.; Kim, J. K.; Park, J. S.; Byun, Y.; Kim, C. K. The Use of Pegylated Liposomes to Prolong Circulation Lifetimes of Tissue Plasminogen Activator. *Biomaterials* **2009**, *30*, 5751−5756.

(28) Woodle, M. C.; Lasic, D. D. Sterically Stabilized Liposomes. *Biochim. Biophys. Acta* **1992**, *1113*, 171−199.
(29) Johnsson, M.; Edwards, K. Liposomes, Disks, and Spherical Micelles: Aggregate Structure in Mixtures of Gel Phase Phosphatidylcholines and Poly(Ethylene Glycol)-Phospholipids. *Biophys. J.* **2003**, *85*, 3839−3847.
(30) Corvalan, N. A.; Clop, E. M.; Perillo, M. A. In *Surface Behaviour of Dipalmitoyl Phosphatidylethanolamine Grafted Poly(Ethylene Glycol) Alone or in Mixtures with Dipalmitoyl Phosphatidylcholine*, XXXVII Reunión Anual de la Sociedad Argentina de Biofísica, La Plata, Buenos Aires, Argentina, Sociedad Argentina de Biología: La Plata, Buenos Aires, Argentina, 2008.
(31) Harris, R. *Nuclear Magnetic Resonance Spectroscopy*; Longman Scientific and Technical: England, 1994; p 250.
(32) Turina, A. V.; Caruso, B.; Yranzo, G. I.; Moyano, E. L.; Perillo, M. A. A Surface Active Benzodiazepine Receptor Ligand for Potential Probing Membrane Order of Gabaa-Receptor Surroundings. *Bioconjugate Chem.* **2008**, *19*, 1888−1895.
(33) Clop, E.; Clop, P.; Sánchez, J. M.; Perillo, M. A. Molecular Packing Tunes in the Kinetics of Beta-Galactosidase Catalized O-Nitrophenyl Galactopiranoside Hydrolysis. *Langmuir* **2008**, *24*, 10950−10960.
(34) Israelachvili, J. N. *Intermolecular and Surface Forces*; Academic Press: New York, 1989.
(35) Clop, E. M.; Corvalan, N. A.; Perillo, M. A. Langmuir Films of Dipalmitoyl Phosphatidylethanolamine Grafted Poly(Ethylene Glycol). In-Situ Evidence of Surface Aggregation at the Air-Water Interface. *Colloids Surf., B* **2013**.
(36) Garcia, D. A.; Perillo, M. A. Flunitrazepam Induces Geometrical Changes at the Lipid−Water Interface. *Colloids Surf., B* **2001**, *20*, 63−72.
(37) Georgiev, G. A.; Sarker, D. K.; Al-Hanbali, O.; Georgiev, G. D.; Lalchev, Z. Effects of Poly (Ethylene Glycol) Chains Conformational Transition on the Properties of Mixed Dmpc/Dmpe-Peg Thin Liquid Films and Monolayers. *Colloids Surf., B* **2007**, *59*, 184−193.
(38) Levstein, P. R.; Gennaro, A. M.; Pincelli, M. M. ^{31}P-NMR and Spin Label EPR as Complementary Techniques for Lipid Polymorphism Studies. In *Recent Research Developments in Biophysical Chemistry*; Condat, C. A., Baruzzi, A. M., Eds.; Research Signpost: Kerala, India, 2002.
(39) Seelig, J. 31p Nuclear Magnetic Resonance and the Head Group Structure of Phospholipids in Membranes. *Biochim. Biophys. Acta* **1978**, *515*, 105−140.
(40) Perillo, M. A.; Scarsdale, N. J.; Yu, R. K.; Maggio, B. Modulation by Gangliosides of the Lamellar-Inverted Micelle (Hexagonal Ii) Phase Transition in Mixtures Containing Phosphatidylethanolamine and Dioleoylglycerol. *Proc. Natl. Acad. Sci. U.S.A.* **1994**, *91*, 10019−10023.
(41) Nguyen, C. T.; Desgranges, F.; Roy, G.; Galanis, N.; Maré, T.; Boucher, S.; Angue Mintsa, H. Temperature and Particle-Size Dependent Viscosity Data for Water-Based Nanofluids − Hysteresis Phenomenon. *Int. J. Heat Fluid Flow* **2007**, *28*, 1492−1506.
(42) Toimil, P.; Prieto, G.; Miñones, J. J.; Sarmiento, F. A Comparative Study of F-Dppc/Dppc Mixed Monolayers. Influence of Subphase Temperature on F-Dppc and Dppc Monolayers. *Phys. Chem. Chem. Phys.* **2010**, *12*, 13323−13332.
(43) Yun, H.; Choi, Y.-W.; Kim, N. J.; Sohn, D. Physicochemical Properties of Phosphatidylcholine (Pc) Monolayers with Different Alkyl Chains, at the Air/Water Interface. *Bull. Korean Chem. Soc.* **2003**, *24*, 377−383.
(44) Milner, S. T. Polymer Brushes. *Science* **1991**, *251*, 905−914.
(45) Lecourtier, J.; Audebert, R.; Quivoron, C. Swelling of Macromolecules Grafted on Inert Surfaces and Partitioning of a Solute between Solvent and Grafted Phase. *Macromolecules* **1979**, *12*, 141−146.
(46) Marsh, D.; Bartucci, R.; Sportelli, L. Lipid Membranes with Grafted Polymers: Physicochemical Aspects. *Biochim. Biophys. Acta* **2003**, *1615*, 33−59.
(47) Sakuragi, M.; Koiwai, K.; Nakamura, K.; Masunaga, H.; Ogawa, H.; Sakurai, K. Transformation from Multilamellar to Unilamellar Vesicles by Addition of a Cationic Lipid to Pegylated Liposomes Explored with Synchrotron Small Angle X-Ray Scattering. *J. Phys.: Conf. Ser.* **2011**, *272*, 012011.
(48) De Vos, C.; Deriemaeker, L.; Finsy, R. Quantitative Assessment of the Conditioning of the Inversion of Quasi-Elastic and Static Light Scattering Data for Particle Size Distributions. *Langmuir* **1996**, *12*, 2630−2636.
(49) Marsh, D. Lateral Pressure in Membranes. *Biochim. Biophys. Acta* **1996**, *1286*, 183−223.